COMMUNICATION

Stable Pseudo[3]rotaxanes with Strong Positive Binding Cooperativity Based on Shape-Persistent Aromatic Oligoamide Macrocycles

Received 00th January 20xx,
Accepted 00th January 20xx

DOI: 10.1039/x0xx00000x

Thomas A. Sobiech,‡[a] Yulong Zhong,‡[a] Laura S. Sánchez B.,[b] Brice Kauffmann,[c] Jillian K. McGrath,[a] Christina Scalzo,[a] Daniel P. Miller,[b] Ivan Huc,[d] Eva Zurek,[a] Yann Ferrand[c] and Bing Gong*[a]

This work is dedicated to Professor David G. Lynn in celebration of his 70th birthday.

New aromatic oligoamide macrocycles with C_3-symmetry bind bipyridinium guest G to form compact pseudo[3]rotaxes involving interesting enthalpic and entropic contributions. The observed high stabilities and strong positive binding cooperativity are found with few other host-guest systems.

Shape-persistent molecular architectures have attracted significant scientific interest as their defined structural characteristics provide unique opportunities for both basic understanding and practical applications.[1] Compared to flexible structures, shape-persistent molecules offer distinctive advantages. Such molecules, with their discrete sizes and defined shapes, engage in predictable intermolecular association and assembly as a result of the cooperative and controlled action of multiple non-covalent forces. By minimizing the energy cost associated with conformational change, shape-persistent foldamers[2] and macrocycles[3] are able to rigidly hold and convergently orient binding sites, based on which hosts containing preorganized cavities with extraordinary guest-binding capabilities are created.

Over the years, we have discovered and studied the six-residue aromatic amide macrocycle **1** and its analogs.[4] Macrocycle **1** has a persistent shape with its backbone being fully constrained due to the presence of highly favorable, three-center intramolecular hydrogen bonds.[5] The internal cavity of **1**, being decorated with six rigidly held amide carbonyl groups that orient toward the center of the macrocycle, is electronegative and capable of strongly binding cationic guests. For example, the guanidinium ion was found to bind tightly with **1**.[6] Guests based on bipyridinium derivatives were found to form 2:1 (host:guest) complexes with **1**.[7] Macrocycle **1** equipped with proper sidechains stacked into membrane-spanning columnar assemblies with electronegative cylindrical inner pores that served as highly conducting channels for cations.[8]

Consisting of alternating diacid and diamine residues derived from the corresponding *meta*-disubstituted benzene derivatives, macrocycle **1** is one of many possible types of aromatic oligoamide macrocycles having constrained backbones. While macrocycles having the same backbone of **1** but differing in sizes have been constructed,[9] adjusting the orientations of the backbone amide groups should lead to new macrocycles that have persistent shapes but with altered backbones and cavities containing varied arrangement of amide oxygen atoms. For example, inverting the orientation of every other backbone amide group of **1** results in macrocycle **2** which has remained unknown until now (Figure 1).

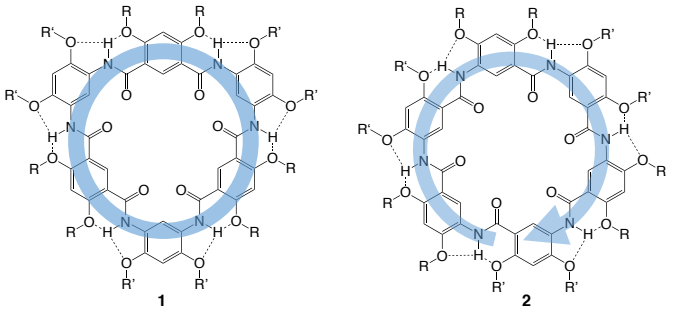

Figure 1. Inverting the orientation of every other backbone amide group of macrocycle **1**, which has a C_2- and C_3-symmetrical backbone highlighted with a blue circle, results in macrocycle **2** which has a C_3-symmetrica (*N*-to-*C*) backbone highlighted with a circular, blue arrow. Hydrogen bonds are shown as dashed lines. R and R' are methyl and other side chains.

Like **1**, macrocycle **2** has an aromatic oligoamide backbone that is fully constrained due to the presence of three-center intramolecular hydrogen bonds. Different from **1**, macrocycle **2** consists of basic residues which share the same core based on 5-amino-2, 4-dialkoxybenzoic acid and thus have the same

[a] *Department of Chemistry, University at Buffalo, the State University of New York, Buffalo, New York 14260, United States.*
[b] *Department of Chemistry 151 Hofstra University 106F Berliner Hall Hempstead, NY 11549, United States.*
[c] *Institut Européen de Chimie et Biologie, UMS3011/US001 CNRS, Inserm, Université de Bordeaux, 2 rue Robert Escarpit, F-33600 Pessac, France .*
[d] *Department Pharmazie, Ludwig-Maximilians-Universität München, Butenandtstraße 5-13, D-81377 Munich, Germany*

†Electronic Supplementary Information (ESI) available. CCDC 2103074. For ESI and crystallographic data in CIF or other electronic format see DOI: See DOI: 10.1039/x0xx00000x

‡These authors contributed equally to this work.

electronic properties. In contrast to macrocycle 1 which has a D_3 symmetry, macrocycle **2** has C_3-symmetry and a backbone with a circular *N*-to-*C*, i.e., clockwise or counterclockwise, direction. With a backbone that is electronically different from that of **1**, macrocycle **2** was expected to have different assembling properties. Besides, the cavity of **2** differs from that of **1** by having convergently oriented, equidistant amide oxygens, which could lead to distinct guest-binding behavior.

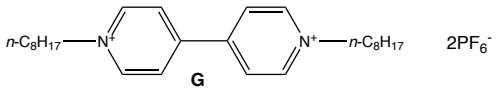

G

Herein we report the synthesis, guest-dependent discrete assembly, and guest-binding of **2**. Guest **G**, derived from the alkylation of 4, 4'-bipyridine with *n*-octyl bromide, followed by exchanging the Br^- with PF_6^- ions, was chosen to examine the capability of **2** in binding cationic species, because similar bipyridinium guests were widely used in assessing the binding capabilities of hosts with electronegative cavities.[10,11]

Our studies revealed that macrocycle **2** bound **G** strongly, with an overall binding constant of over 10^{11} M^{-2} and a 2:1 stoichiometry in the polar solvent DMSO/$CHCl_3$ (1/1, v/v). The formation of the 2:1 complexes, as highly stable pseudo[3]rotaxanes,[12] shows very strong positive cooperativity, with the second binding even being much more favorable then the first one. X-ray structure reveals a highly compact pseudo[3]rotaxane in which the two molecules of **2** undergo strong aromatic stacking with their backbones following the same, i.e., clockwise or counterclockwise, *N*-to-*C* direction.

Scheme 1. Synthesis of macrocycles **2a** and **2b**

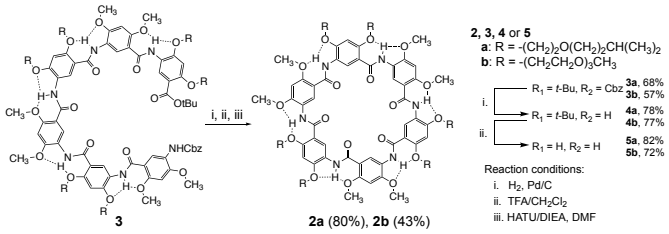

Macrocycles **2a** and **2b** were synthesized from noncyclic **3a** and **3b** which are members of aromatic oligoamide foldamers we developed over the years.[13] Removing the CBZ and *t*-butyl groups from oligoamides **3a** and **3b** gave the amine- and carboxyl-terminated hexamers which, with constrained backbones enforcing stably folded, crescent conformations, were predisposed to cyclization. Macrocycles **2a** and **2b** were obtained in good to excellent isolated yields (from 43% to 80%) by treating the corresponding linear hexamers with the coupling reagent 1-[Bis(dimethylamino)methylene]-1H-1,2,3-triazolo[4,5-b]pyridinium 3-oxide hexafluorophosphate (HATU).

The proton resonances of **2a** (1 mM) appear as featureless broad peaks in $CDCl_3$, suggesting self-aggregation that restricts the motion of the macrocyclic molecules. Adding DMSO-d_6 to $CDCl_3$ resulted in the sharpening and downfield shifting of ^{1}H NMR signals, with the ^{1}H NMR peaks becoming well dispersed upon increasing the ratio of DMSO-d_6 to 20% (by volume) or more. The NMR signals continued to sharpen and shift downfield with increasing ratio of DMSO-d_6, indicating the weakening of aggregation and aromatic stacking interactions in solvents of enhanced polarity (Figure S1). With 50% (by volume) or more DMSO-d_6 in $CDCl_3$, the line width of NMR peaks ceased to change, which points to the complete interruption of aggregation. In DMSO-d_6/$CDCl_3$ (1/1, v/v), the ^{1}H NMR resonances of **2a** from 1 mM to 0.05 mM remain unchanged in both their line width and chemical shifts (Figure S2), demonstrating that **2a** became molecularly dissolved.

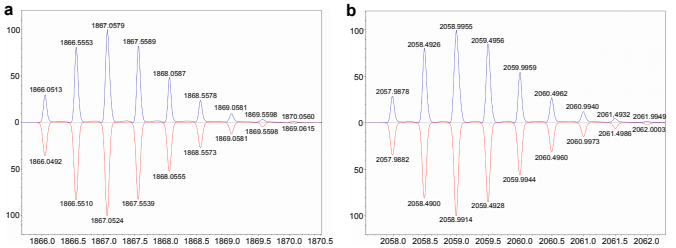

Figure 2. Isotope distributions of (**a**) the $[\mathbf{2a} + \mathbf{G} + \mathbf{2a}]^{2+}$ and (**b**) $[\mathbf{2b} + \mathbf{G} + \mathbf{2b}]^{2+}$ ions from ESI-Q-TOF (blue) and computer simulation (red).

Examining the mixture of **2a** or **2b** and **G** with Electrospray-ionisation quadrupole time-of-flight mass spectrometry (ESI-Q-TOF) revealed ions with mass/charge ratios at 1867.0657 and 2058.9883, respectively, that appear as the base peaks in the mass spectra (Figure S3). These peaks correspond to the 2:1 complexes of **2a** and **2b** with **G**, i.e., pseudo[3]rotaxes, as confirmed by the excellent match of the measured and simulated isotope distributions (Figure 2). Ions corresponding to the 1:1 complexes of **2a** and **2b** with **G**, with mass/charge ratios of 1029.1089 and 1125.0772, respectively, only appear as minor peaks in the mass spectra (Figure S3). These results indicate that **2a** and **2b** bind **G** strongly in a 2:1 stoichiometry. The fact that the ions corresponding to the 2:1 complexes give rise to the most prominent peaks in the mass spectra demonstrate the high stabilities of the pseudo[3]rotaxanes.

Mixing the solutions of **2a** and **G**, both being colorless, gave a solution that turned light yellow. This observation prompted us to examine the binding of **2a** with **G** with UV-vis titration in DMSO/$CHCl_3$ (1/1, v/v).† Plotting the change in the absorbance of **2a** (1 mM) at 430 nm against the proportions of **G** (0 to 2 equiv) revealed two distinct trend lines showing an abrupt change in their slopes at ~0.5 equiv of **G** (Figure S4), which confirms the 2:1 binding of **2a** and **G** revealed by ESI. The abrupt change indicates a proper titration regime at the concentration of this experiment. Thus, efforts to fit the UV-vis titration data failed to yield satisfactory results due to large errors.

To gain additional insights into the host-guest interaction between macrocycle **2** and guest **G**, the affinities of **2a** and **2b** for **G**, along with other thermodynamic parameters of the binding events, were determined with (Isothermal titration calorimetry, ITC) titration experiments. In DMSO/$CHCl_3$ (1/1, v/v), both **2a** and **2b** bind **G** in high binding affinities, with the overall binding constants being around 10^{11} M^{-2} (Table 1).

The stepwise binding constants K_1 and K_2, along with the corresponding enthalpy and entropy changes, reveal interesting similarity and difference between the two host-guest pairs (Table 1 and Figure S5). Differing only in their side chains, macrocycles **2a** and **2b** show different details in their binding of **G**. For both complexes, the first and second binding events are entropically and enthalpically driven, respectively. The first binding events of **2a** and **2b** with **G**, being both entropically dominant, involve opposite enthalpic contributions. That of **2a** is enthalpically favorable and that of **2b** is unfavorable. In contrast, the second binding events of **2a** and **2b** with **G**, being both enthalpically dominant, involve opposite entropic contributions. That of **2a** is entropically favorable and that of **2b** is unfavorable. The observed difference in the behavior of **2a** and **2b** may be due to different solvation of these two macrocycles, which only differ in their sidechains that may lead to different enthalpic and entropic outcomes. The specific factors responsible for the observed difference remain to be elucidated, which requires additional systematic studies.

Table 1. Thermodynamic Parameters, Binding Constants and Interaction Parameters (α) for the 2:1 complexes of hosts **2a** and **2b** with guest **G**.[a]

	2a	**2b**
ΔH_1 (cal/mol)	(-1.94 ± 0.31) x 10^3	(5.97 ± 2.29) x 10^3
$T\Delta S_1$ (cal/mol)	(5.18 ± 2.21) x 10^3	(12.5 ± 2.87) x 10^3
K_1 (M^{-1})	(1.69 ± 0.52) x 10^5	(6.41 ± 1.70) x 10^4
ΔH_2 (cal/mol)	(-5.16 ± 0.29) x 10^3	(-14.7 ± 2.30) x 10^3
$T\Delta S_2$ (cal/mol)	(3.37 ± 2.07) x 10^3	(-6.31 ± 3.14) x 10^3
K_2 (M^{-1})	(1.79 ± 0.43) x 10^6	(1.47 ± 0.38) x 10^6
K_{total} (M^{-2})	(3.03 ± 1.18) x 10^{11}	(9.42 ± 3.49) x 10^{10}
α^b	42	92

[a]The data here are a summary of binding data obtained from ITC titrations of **2a** (450 μM) or **2b** (450 μM) into **G** (25 μM) in DMSO/$CHCl_3$ (1/1, v/v) at 25 °C. [b]The interaction parameter $\alpha = 4K_2/K_1$ (α > 1: positive cooperativity; α < 1: negative cooperativity; α = 1: no cooperativity).[14]

For both complexes, the K_2 values are 10 to 20 times greater than the K_1 values. Thus, for **2a** or **2b**, the second molecule binds to **G** in much higher affinity than the first one does. As indicated by the interaction parameters α of 42 and 92,[14] respectively, for **2a** and **2b**, the formation of the pseudo[3]rotaxanes involves fairly strong positive cooperativity.

Differing from that of **1**, the oligoamide backbone of **2a** and **2b** seems to have a higher propensity for intermacrocyclic stacking interactions, which, along with electrostatic and perhaps C-H•••O hydrogen-bonding interactions between the host and guest, promotes the binding of the second macrocycle and the positive cooperativity in the binding of **G** to **2a** or **2b**.

Single crystals, obtained by slow liquid–liquid diffusion of CH_3OH into a solution of **2a** and **G** in CH_2Cl_2, provided the crystal structure of pseudo[3]rotaxane **$2a_2$•G** (Figure 3). Guest **G** threads through the 8.2-Å (or 5.1-Å vdw) cavities of the macrocycles, with the long axis of its bipyridinium unit being titled at an angle of ~45° to the C_3 axis of symmetry of each macrocycles. The bipyridinium CH groups engage in C-H•••O interactions, with each of the pyridinium rings forming C-H•••O bonds with four of the six amide O atoms of each macrocycle.

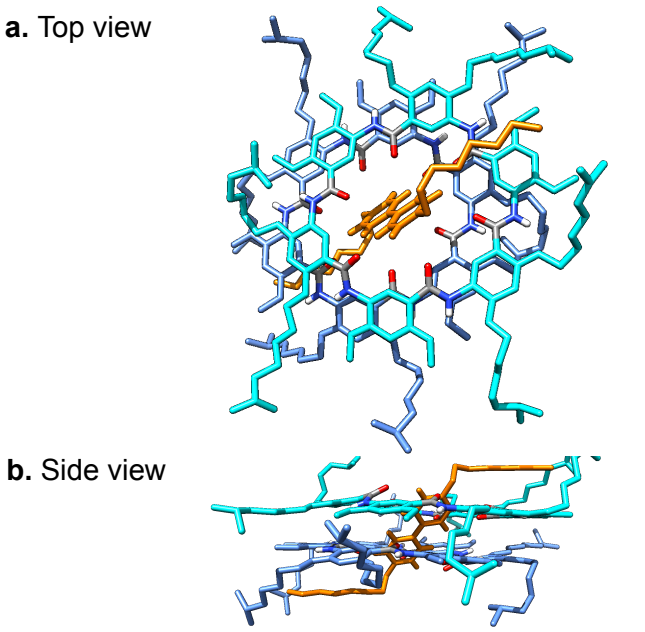

Figure 3. Crystal structure of pseuo[3]rotaxane **$2a_2$•G**. PF_6^- ions and hydrogen atoms except for those of the bipyridinium unit of **G** and the amide groups of **2a** are omitted. Amide groups are shown by element colour to indicate backbone orientation. **G** is shown in orange. The two molecules of **2a** are shown in cyan and cornflower blue, respectively.

N^+•••O distances of 3.23 Å and 3.46 Å were found between each of the pyridinium N atoms and two amide O atoms of one of the two macrocycles, indicative of strong charge-dipole interactions. Each of the two octyl "tails" of **G** is in van der Waals contact distances with an aromatic residue from one of the two macrocycles, which caps the dimeric stack of **2a** (Figure 3b).

In addition to the observed interactions between **2a** and **G**, the two macrocycles in the pseudo[3]rotaxane adopt nearly planar conformations and are in close contact, with inter-macrocyclic stacking distances between 3.4 and 3.5 Å, indicating very strong stacking interactions. The two macrocycles in **$2a_2$•G** are offset and have their backbone in the same clockwise (or counterclockwise) *N*-to-*C* direction. The other possible arrangement of the two macrocycles, one with its backbone being in a clockwise and the other in a counterclockwise direction, is absent in the X-ray structure.

Thus, the X-ray structure reveals the atomic details of a compact complex of **2a** and **G** in which the bipyridinium segment of guest **G** is completely encapsulated in the cavities of two stacked molecules of **2a**, which, along with the van der Waals contacts between the octyl end groups and the backbone aromatic residues of **2a**, results in maximum contact between **2a** and **G**. Strong stacking between the two molecules of **2a** provide additional stabilization for the complex, leading to the strong cooperativity observed in the binding of **2** and **G**.

The interaction parameters α of 42 and 92 observed with the binding of **2a** or **2b** with **G** reveal strong positive cooperativity. In contrast, the binding of macrocycle **1** with bipyridinium guests showed negative to weakly positive cooperativity with

the largest α value being 2.5.[7] Such a noticeable cooperativity was probed by performing density functional theory calculations on the binding of **2** with **G**.[15] The optimized structure of complex $\mathbf{2_2}$•**G** (Figure 4, left) closely resembles the crystal structure of $\mathbf{2a_2}$•**G**, indicating the reliability of our method. The interaction energy,† which reflects the binding between **2** and **G**, of complex $\mathbf{2_2}$•**G** is much larger in magnitude than the that of binding one molecule of **2** to **G** (Figure 4, right). These results show that the second binding event is energetically highly favorable, which is in line with the experimentally observed strong positive cooperativity in the binding of **G** with **2**.

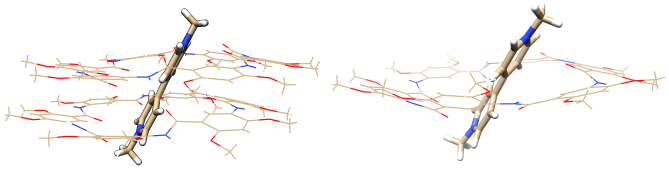

Figure 4. Energy-minimized structures of the 2:1 complex $\mathbf{2_2}$•**G** (left) and 1:1 complex **2**•**G** (right) DMSO/$CHCl_3$ (1/1). The octyl end groups of guest **G** and the R side chains of **2** are replaced with methyl groups in the computed structures. Interaction energies† are shown underneath the structures.

In summary, macrocycles **2a** and **2b** were found to strongly bind to bipyridinium guest **G** in a 2:1 stoichiometry, forming highly stable pseudo[3]rotaxanes. Results from ITC titrations reveal that the interaction of **2** with **G** is featured by strong overall binding, different dominant entropic or enthalpic factors associated with the first and second binding events, and most prominently, much stronger positive cooperativities than those observed with other aromatic oligoamide macrocycles of comparable sizes. The X-ray structure of pseudorotaxane $\mathbf{2a_2}$•**G** reveals a compact assembly that is stabilized by hydrogen-bonding, charge-dipole, aromatic stacking, and van der Waals interactions. Computational studies revealed drastically enhanced interaction for the 2:1 complex over that of the 1:1 complex, which further demonstrates the strong positive cooperativity of this system. Macrocycle **2** represents a new member of aromatic oligoamide macrocycles, based on which highly stable pseudorotaxanes are being developed.

This research was supported by the American Chemical Society–Petroleum Research Fund (PRF No. 58364-ND7 to B. G.), the US National Science Foundation (CHE-1905094 and 2108538 to B. G. and CHE-2108597 to D. P. M.).

Author contributions

Synthesis and characterization (T. A. S., Y. L., J. K. M., C. S.); computation (L. S. S. B., D. P. M., E. Z.); X-ray crystallography (B. K., Y. F., I. H.); general discussion (T. A. S., Y. L. Z., D. P. M., I. H., E. Z., Y. F., B. G.); Design and manuscript writing (B. G.).

Conflicts of interest

There are no conflicts to declare.

Notes and references

1. (a) J. L. Sessler and A. K. Burrell, *Top. Curr. Chem*. 1992, **161**, 177. (b) J. S. Moore, *Acc. Chem. Res.* 1997, **10**, 402. (c) B. Gong, *Chem. Eur. J*. 2001, **7**, 4336. (d) S. Höger, *Chem. Eur. J*. 2004, **10,** 1320. (e) H. Juwarker and K. -S. Jeong, *Chem. Soc. Rev*. 2010, **39**, 3664. (f) K. P. McDonald, Y. R. Hua, S. Lee and A. H. Flood, *Chem. Commun.,* 2012, **48**, 5065. (g) T. Ogoshi, T.-A. Yamagishi and Y. Nakamoto, *Chem. Rev.* 2016, **116**, 7937.
2. (a) J. Zhu, R. D. Parra, H. Q. Zeng, E. Skrzypczak-Jankun, Martinovic, X. C. Zeng and B. Gong, *J. Am. Chem. Soc.* 2000, **122**, 4219. (b) H. Jiang, J.-M. Léger and I. Huc, *J. Am. Chem. Soc*. 2003, **125**, 3448. (c) J.-L. Hou, X.-B. Shao, G.-J. Chen, Y.-X. Zhou, X.-K. Jiang and Z.-T. Li, *J. Am. Chem. Soc.* 2004, **126**, 39, 12386. (d) K. J. Chang, B. N. Kang, M. H. Lee and K. -S. Jeong, *J. Am. Chem. Soc*. 2005, **127**, 12214. (e) Y. Yan, B. Qin, C. L. Ren, X. Y. Chen, Y. K. Yip, R. J. Ye, D. W. Zhang, H. B. Su and H. Q. Zeng, *J. Am. Chem. Soc*. 2010, **132**, 5869. (f) Y. R. Hua, Y. Liu, C. H. Chen and A. H. Flood, *J. Am. Chem. Soc*. 2013, **135**, 14401. (g) C. J. Massena, N. B. Wageling, D. A. Decato, E. M. Rodriguez, A. M. Rose and O. B. Berryman, *Angew. Chem., Int. Ed*. 2016, **55**, 12398.
3. (a) J. L. Sessler, S. J. Weghorn, T. Morishima, M. Rosingana, V. Lynch and V. Lee, *J. Am. Chem. Soc.* 1992*,* **114**, 8306. (b) K. H. Choi and A. D. Hamilton, *J. Am. Chem. Soc*. 2001, **123**, 2456. (c) L. He, Y. An, L. H. Yuan, W. Feng, M. F. Li, D. C. Zhang, K. Yamato, C. Zheng, X. C. Zeng and B. Gong, *Proc. Natl. Acad. Sci. U. S. A*. 2006, **103**, 10850. (d) S. J. Brooks, P. A. Gale and M. E. Light, *Chem. Commun.*, 2006, **41**, 4344. (e) H. L. Fu, Y. Liu and H. Q. Zeng, *Chem. Commun.,* 2013*,* **49**, 4127. (f) J. H. Oh, J. H. Kim, D. S. Kim, H. J. Han, V. M. Lynch, J. L. Sessler and S. K. Kim, *Org. Lett.*, 2019, **21**, 4336.
4. L. H. Yuan, W. Feng, K. Yamato, A. R. Sanford, D. G. Xu, H. Guo and B. Gong, *J. Am. Chem. Soc.* 2004, **126**, 11120.
5. R. D. Parra, H. Q. Zeng, J. Zhu, C. Zheng, X. C. Zeng and B. Gong, *Chem. Eur. J*. 2001, **7**, 4352.
6. A. R. Sanford, L. H. Yuan, W. Feng, K. Yamato, R. A. Flowers and B. Gong, *Chem. Commun.* 2005, 4720.
7. X.W. Li, X. Y. Yuan, P.C. Deng, L.X. Chen, Y. Ren, C. Y. Wang, L. X. Wu, W. Feng, B. Gong and L. H. Yuan, *Chem. Sci*. 2017, **8**, 2091.
8. A. J. Helsel, A. L. Brown, K. Yamato, W. Feng, L. H. Yuan, A. Clements, S. V. Harding, G. Szabo, Z. F. Shao and B. Gong, *J. Am. Chem. Soc*. 2008, **130**, 15784.
9. W. Feng, L. Yamato, L.Q. Yang, J. Ferguson, L. J. Zhong, S. L. Zou, L. H. Yuan, X. C. Zeng and Gong, B. *J. Am. Chem. Soc*. 2009, **131**, 2629.
10. (a) M. M. Zhang, K. L. Zhu and F. H. Huang, *Chem. Commun*., 2010, **46**, 8131. (b) A. Trabolsi, *Nat. Rev. Chem*. 2021, **5**, 442.
11. W. Ong, M. Gómez-Kaifer and A. E. Kaifer, *Org. Lett.* 2002, **4**, 1791. (b) K. Moon and E. Kaifer, *Org. Lett.*, 2004, **6**, 185. (c) T. Ogoshi, M. Hashizume, T. Yamagishi and Y. Nakamoto, *Chem. Commun.*, 2010, **46**, 3708. (d) N. K. Beyeh, H. H. Jo, I. Kolesnichenko, F. Pan, E. Kalenius, E. V. Anslyn, R. H. A. Ras and K. Rissanen, *J. Org. Chem.*, 2017, **82**, 5198.
12. M. Xue, Y. Yang, X. D. Chi, X. Z. Yan, F. H. Huang, *Chem. Rev.* **2015**, *115*, 7398.
13. L. H. Yuan, A. R. Sanford, W. Feng, A. M. Zhang, J. S. Ferguson, K. Yamato, J. Zhu, H. Q. Zeng and B. Gong, *J. Org. Chem*. **2005**, *70*, 10660.
14. (a) K. A. Connors, A. Paulson and D. Toledo-Velasquez, *J. Org. Chem*., 1988, **53**, 2023. (b) Hunter, C. A.; Anderson, H. L. What is cooperativity? *Angew. Chem., Int. Ed*. 2009, **48**, 7488. (c) P. Thordarson, *Chem. Soc. Rev*. 2011, **40**, 1305.
15. G. te Velde, F. M. Bickelhaupt, E. J. Baerends, C. Fonseca Guerra, S. J. A. van Gisbergen, J. G. Snijders and T. Ziegler, *J. Comput. Chem*. 2001, **22**, 931.